



# A fluorescent peptidyl substrate for visualizing peptidyl-prolyl *cis/trans* isomerase activity in live cells†

Cite this: *Chem. Commun.*, 2018, 54, 1857

Received 28th November 2017,  
Accepted 23rd January 2018

DOI: 10.1039/c7cc09135d

rsc.li/chemcomm

Quan Jiang,<sup>‡a</sup> Xiao-Rong Li,<sup>‡a</sup> Cheng-Kun Wang,<sup>a</sup> Juan Cheng,<sup>a</sup> Chao Tan,<sup>a</sup> Tian-Tian Cui,<sup>a</sup> Nan-Nan Lu,<sup>a</sup> Tony D. James,<sup>id b</sup> Feng Han<sup>\*a</sup> and Xin Li<sup>id \*a</sup>

**This communication reports on a fluorescent probe (PPI-P) for imaging active peptidyl-prolyl *cis/trans* isomerases in live cells. PPI-P is capable of responding to both recombinant and cellular PPIases fluorogenically, and has been shown to specifically image active PPIases in live cells.**

Due to the partial double bond character of peptidyl-prolyl bonds and the high activation enthalpies for *cis/trans* isomerization, prolyl isomerization is intrinsically slow but can be accelerated by peptidyl-prolyl *cis/trans* isomerases (PPIases).<sup>1</sup> PPIases are therefore considered as important chaperones in modulating the folding, trafficking and function of target proteins.<sup>2–4</sup> PPIases are divided into three groups, the FK506-binding proteins (FKBP), Cyclophilin and the Parvulins (Pin1 and Par14).<sup>5,6</sup> PPIases directly or indirectly regulate pathogenic protein multimerization in human diseases and represent a family rich in targets for modulating mitochondrial function, chaperone activity, stress response, transcription gene regulation, chromatin dynamic, and kinase activity.<sup>7–11</sup> Many individual genes within the PPIase family are associated with age-related diseases,<sup>12</sup> including cardiovascular diseases, cancer and age-related macular degeneration, *e.g.*, Pin1 has been implicated in the pathogenesis of cancers and Alzheimer's disease,<sup>13,14</sup> while FKBP25 participates in the epigenetic regulation of gene expression and ribonucleoprotein complexes.<sup>15</sup> Despite the biological importance, the relationship between PPIase activities and their precise function, and the underlying mechanism responsible for physiological regulation and pathological dysregulation of prolyl isomerization remain largely unknown, which emphasizes the necessity for reliable assays for monitoring PPIase activity.

To date, the catalytic activity of PPIases has usually been monitored spectrophotometrically *via* the chymotrypsin-coupled assay using *N*-succinyl-Ala-Ala-Pro-Phe-*p*-nitroanilide peptide as a probe. This assay exploits the finding that  $\alpha$ -chymotrypsin can proteolyze the *p*-nitroanilide amide bond to enhance the absorbance at 390 nm when the Ala-Pro bond is in the *trans* conformation.<sup>16,17</sup> While this assay has facilitated PPIase evaluation and yielded important results, it can only be used with lysates or recombinant proteins, thus precluding the application to live cells. Since cell lysis disrupts the carefully controlled cellular environment and may affect the stability and function of target proteins, it is very important to study proteins in their native environments in order to achieve more biologically relevant results.<sup>18</sup>

In recent years, chemical tools have become the method of choice for detecting protein activity in intact live samples.<sup>19,20</sup> Although there have been a number of probes reported for imaging various proteins, probes that could significantly advance PPIase research remain undeveloped. With this research we introduce an exciting new chemical tool to the currently available toolbox of probes dedicated to understanding protein function: a fluorogenic probe (**PPI-P**) for monitoring PPIase activity in live cells. The probe is a peptide with the sequence of Ala-Ala-Pro-Phe labeled with a 6-(dimethylamino)-2-naphthoyl fluorophore at the N terminus and a *p*-nitroanilide group at the C terminus. We reasoned that the *cis* geometry of **PPI-P** would bring the naphthalene fluorophore and the nitroanilide quencher into close proximity and therefore cause fluorescence quenching.<sup>21</sup> Prolyl isomerases can catalyze the transformation of the *cis* prolyl bond to *trans*, separating the fluorophore from the quencher and therefore restoring the fluorescence. We have shown that **PPI-P** is sensitive to PPIases *in vitro*. Notably, it facilitates the visualization of the dynamic changes involved during PPIase activity in live cells.

Initially, to facilitate the imaging of functional PPIases in live cells, we took advantage of their ability to catalyze prolyl-containing peptide isomerization. Since the distance between the N and C terminals of a peptide may change significantly

<sup>a</sup> College of Pharmaceutical Sciences, Zhejiang University, Hangzhou 310058, China. E-mail: changhuahan@zju.edu.cn, lixin81@zju.edu.cn

<sup>b</sup> Department of Chemistry, University of Bath, Bath, BA2 7AY, UK

† Electronic supplementary information (ESI) available. See DOI: 10.1039/c7cc09135d

‡ These authors contributed equally to this work.

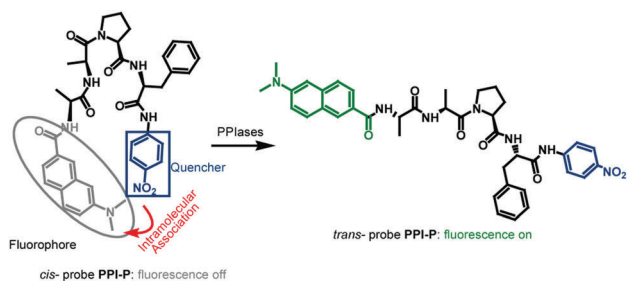


Fig. 1 Structure of PPI-P and the proposed mode of action.

before and after the peptidyl-prolyl isomerization, a fluorophore and a quencher were incorporated into a PPIase substrate, resulting in a probe where fluorescence intensity changes can be used to monitor the isomerization. For this purpose, Ala-Ala-Pro-Phe was selected as a representative PPIase substrate due to its broad-spectrum activity among various PPIases,<sup>22</sup> and the probe PPI-P was developed by tagging the tetrapeptide with the 6-(dimethylamino)-2-naphthoyl fluorophore at the N terminus and the *p*-nitroanilide quencher at the C terminus. We reasoned that as the *cis* isomer, the probe would be weakly fluorescent due to the close proximity of the fluorophore and the quencher. Then, PPIases would catalyze the isomerization from *cis* to *trans*, separating the fluorophore from the quencher, resulting in a concomitant fluorescence increase (Fig. 1). The tagged PPI-P peptide was synthesized as detailed in the ESI†. As shown by the attached NMR traces in the ESI†, both the <sup>1</sup>H NMR signals and <sup>13</sup>C NMR signals of PPI-P appear in pairs, suggesting the presence of both the *cis* and *trans* isomers. However, high performance liquid chromatography (HPLC) analysis gave only one peak under several elution conditions. After failing to differentiate the *cis* isomer from the *trans* one, we decided to use PPI-P as such for the following experiments.

With PPI-P in hand, we first investigated its fluorescence response towards PPIases in lysates. Given that PPIases exist in most cell types, we then measured the fluorescence response of PPI-P to various lysates. Having confirmed that the lysis buffer caused no change to the PPI-P fluorescence (Fig. S1, ESI†), we then recorded the spectra of PPI-P in the presence of various lysates. As shown in Fig. 2A, PPI-P itself in PBS displayed moderate fluorescence centered at 460 nm ( $\lambda_{\text{max}}$  0.101), probably due to the presence of residual *trans* isomer. Interestingly, all the cell lysates tested were able to induce fluorescence enhancement of PPI-P. And an increase of the fluorescence quantum yield to 0.132 was observed when the PPI-P fluorescence plateaued after the treatment of lysate from HEK-293 cells. Furthermore, using lysate from N2a cells, we were able to demonstrate that the fluorescence increase of PPI-P was dose dependent, with increasing lysate resulting in a stronger fluorescence response (Fig. 2B and Fig. S2, ESI†), and similar results were obtained when PPI-P was treated with the lysate from HEK-293 cells (Fig. S3, ESI†). To make sure that this observed fluorogenic response towards cell lysates was not due to probe aggregation, we determined the solubility of PPI-P in PBS (pH 7.4, 10 mM) *via* UV absorption analysis, and a linear

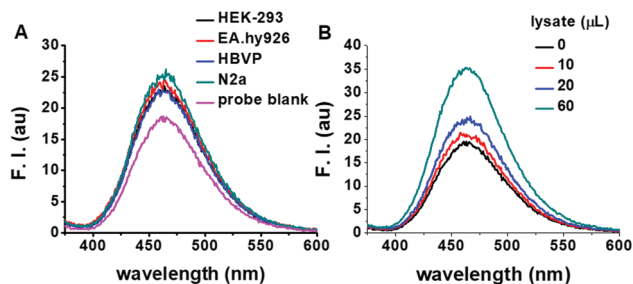
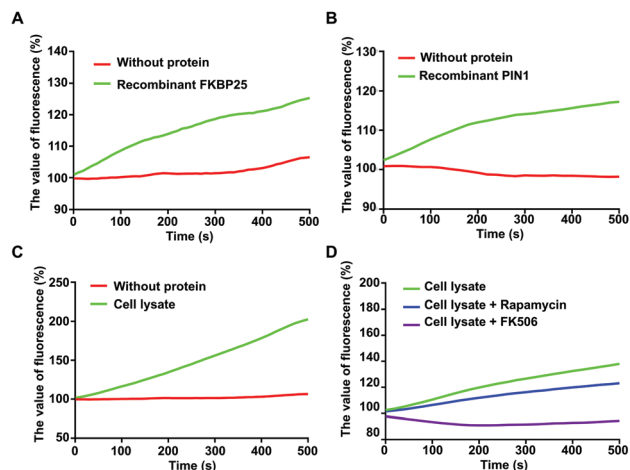


Fig. 2 (A) Fluorescence spectra of PPI-P (5 μM) before and after the treatment (10 min) of lysates (20 μL) from various cell lines. (B) Fluorescence spectra of PPI-P (5 μM) after the treatment (10 min) of various amounts of lysate from N2a cells. All cell lysates were adjusted to a total protein concentration of 1 μg μL<sup>-1</sup> before addition. Spectra were taken in PBS (10 mM, pH 7.4) at ambient temperature.

correlation between the absorption intensity and the PPI-P concentration was observed in the range of 0–50 μM (Fig. S4, ESI†), suggesting the good solubility of the probe under the working concentration. We also confirmed that PPI-P was stable in the cell lysate by monitoring the probe-lysate mixture with liquid chromatography-mass spectrometry (LC-MS) analysis. As shown in Fig. S5 (ESI†), when PPI-P was treated with the HEK-293 lysate, a time-dependent fluorescence intensification was observed. When aliquots of the mixture at an indicated time were analysed using LC-MS, no new peak other than that of PPI-P could be found, indicating that PPI-P is stable enough to resist decomposition at least during the tested period. These results also indicate that the fluorogenic response of PPI-P towards cell lysates was due to its isomerization from *cis* to *trans*.

To further confirm that the fluorescence response of PPI-P to cell lysates was due to PPIases, two additional experiments were performed. First, the response of PPI-P towards recombinant PPIases was investigated. For this purpose, recombinant FKBP25 and Pin1 were chosen due to their relevance in the pathological processes of cardiovascular and cerebrovascular disorders.<sup>23,24</sup> The catalytic activity of FKBP25 was verified using the traditional chymotrypsin-coupled assay which displayed a dramatically accelerated enhancement for the absorption of *N*-succinyl-Ala-Ala-Pro-Phe-*p*-nitroanilide at 405 nm in the co-presence of  $\alpha$ -chymotrypsin (Fig. S6, ESI†), indicating the efficient catalytic activity of recombinant FKBP25. Interestingly, when the PPI-P probe was treated with the same recombinant FKBP25, a significant fluorescence enhancement was observed (Fig. 3A). Consistently, similar results were obtained for recombinant Pin1 treatment (Fig. 3B), demonstrating the potential of PPI-P as a reliable and facile probe for PPIase activity.

Second, we investigated the effect of FKBP inhibitors on the lysate-induced fluorescence enhancement. When PPI-P was treated with the whole lysate derived from HEK293 cells, a significant fluorescence enhancement was observed (Fig. 3C). However, the fluorescence increase was significantly reduced when the system was co-incubated with rapamycin or FK506, two potent inhibitors of FKBP (Fig. 3D), clearly suggestive of PPI-P being the molecular target of PPIases. All these results



**Fig. 3** Characterization of the kinetic response of **PPI-P** to PPIases. **PPI-P** fluorescence was recorded at 460 nm after recombinant FKBP25 ( $1 \mu\text{g } \mu\text{L}^{-1}$ ,  $10 \mu\text{L}$ ) (A) or recombinant Pin1 ( $1 \mu\text{g } \mu\text{L}^{-1}$ ,  $10 \mu\text{L}$ ) (B) treatment. (C) Lysate from HEK293 cells ( $1 \mu\text{g } \mu\text{L}^{-1}$ ,  $10 \mu\text{L}$ ) could also induce a **PPI-P** fluorescence increase and (D) this increase by cell lysate ( $1 \mu\text{g } \mu\text{L}^{-1}$ ,  $5 \mu\text{L}$ ) could be blocked in the presence of the FKBP inhibitor rapamycin (final concentration,  $10 \mu\text{M}$ ) and FK506 (final concentration,  $1 \text{ mM}$ ).

taken together demonstrate the specificity of **PPI-P** towards PPIases among the myriad of other biological components found in lysates.

Having confirmed the capability of **PPI-P** to evaluate the PPIase activity from lysates, we moved on to evaluate the feasibility to image endogenous PPIase activity in live cells. We first confirmed that **PPI-P** had little cytotoxicity by CCK-8 assay (Fig. S7, ESI†). Then we stained EA.hy926 cells with **PPI-P** after the cells were transfected with lentiviral vector encoding EGFP for dual-colour confocal imaging, and the dynamic change of **PPI-P** fluorescence in the transfected cells was monitored (video S1, ESI†).

The series of images in Fig. 4A are individual frames from the continuous time-lapse movie, from which we observed the gradual elevation of intracellular **PPI-P** fluorescence in a time dependent manner, which was confirmed by quantification of the fluorescence data (Fig. S8, ESI†), indicating the presence of native PPIases and their catalytic effect on **PPI-P** to catalyze the isomerization of the probe from *cis* to *trans*. In order to assess the specificity of **PPI-P** in live cells, its fluorescence response in EA.hy926 cells pretreated with rapamycin was monitored (video S2, ESI†). As shown in Fig. 4B and Fig. S8 (ESI†), PPIase inhibition by rapamycin resulted in a reduced and delayed fluorescence response for **PPI-P** to endogenous PPIases, further demonstrating the specificity of **PPI-P** for PPIases in live cells.

To further evaluate the spatiotemporal resolution of **PPI-P** for determining PPIase activity in live cells, the response towards overexpressed FKBP25 fused with EGFP was investigated. The lentivirus vector encoding EGFP-FKBP25 was transfected into live EA.hy926 cells, and FKBP25-overexpression-induced **PPI-P** fluorescence changes were monitored in real-time with EGFP as an overexpression indicator (video S3, ESI†). Representative images from video S3 (ESI†) are given in Fig. 5.

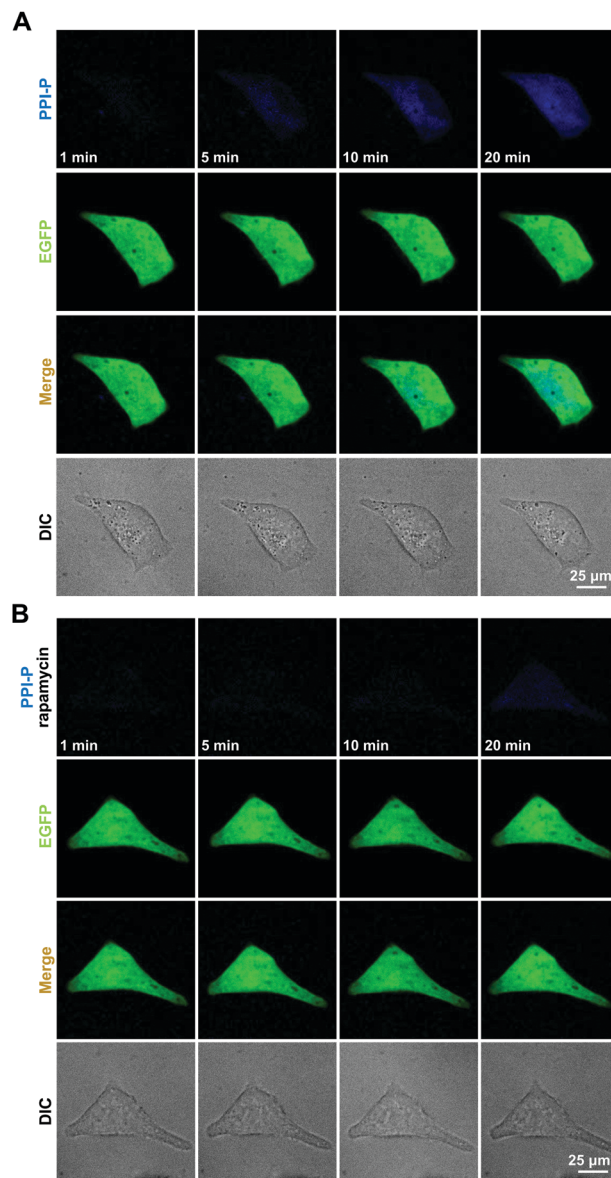


**Fig. 4** Detection of endogenous PPIase activity in live EA.hy926 cells with **PPI-P**. Data shown are the time-lapse confocal images of EA.hy926 cells treated with **PPI-P** (final concentration,  $2.5 \mu\text{M}$ ) in the absence (A) or presence (B) of rapamycin (final concentration,  $1 \mu\text{M}$ ). Lentiviral vector encoding EGFP was transfected into EA.hy926 cells for confocal imaging. The merge panels indicate an overlap of the EGFP (green) signal with the **PPI-P** (blue) signal. Probe fluorescence was collected at  $420\text{--}480 \text{ nm}$  with  $\lambda_{\text{ex}} = 405 \text{ nm}$ . EGFP fluorescence was collected at  $500\text{--}550 \text{ nm}$  with  $\lambda_{\text{ex}} = 488 \text{ nm}$ .

Notably, the intracellular **PPI-P** fluorescence was positively correlated with the FKBP25 expression level with cells over-expressing EGFP-FKBP25 demonstrating stronger **PPI-P** fluorescence than their non-overexpressing counterparts (Fig. 5 and Fig. S9, ESI†), which agrees well with the data in Fig. 2B, further suggesting the specificity of **PPI-P** towards PPIases. Taken together, these experiments provide convincing evidence that **PPI-P** is capable of detecting endogenous PPIase activity in live cells.



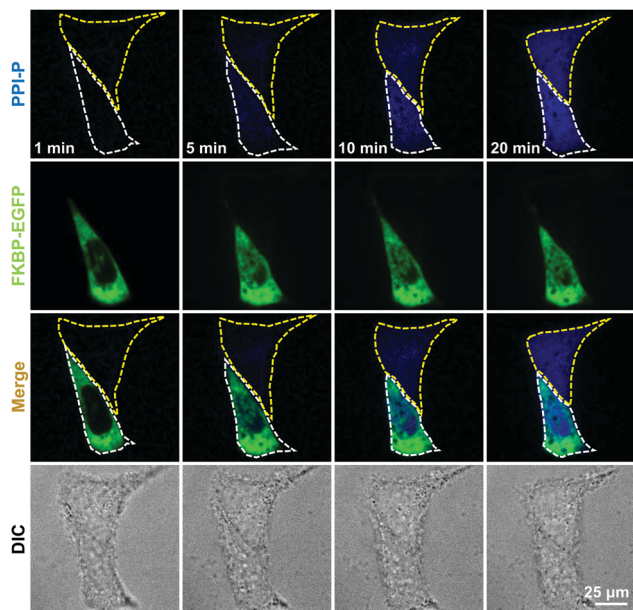


**Fig. 5** Confocal fluorescence images of FKBP25-induced PPIase activity detected by **PPI-P** in live EA.hy926 cells. Lentiviral vector encoding FKBP25-EGFP was transfected into EA.hy926 cells. Cells were then treated with **PPI-P** (2.5  $\mu$ M). Data shown are the time-lapse series for confocal plane images recorded from live EA.hy926 cells over a 20 min time frame. The dashed lines in white or yellow respectively indicate the cells over-expression the FKBP25-EGFP or not. Probe fluorescence was collected at 420–480 nm with  $\lambda_{\text{ex}}$  = 405 nm. EGFP fluorescence was collected at 500–550 nm with  $\lambda_{\text{ex}}$  = 488 nm.

In summary, by taking advantage of the mechanism of PPIase activity, we have developed a fluorogenic probe to report on the catalytic activity of PPIases in both lysates and live cells. The specificity and sensitivity of the probe have been demonstrated using the imaging of exogenous and endogenous PPIases in live cells. It should be noted that although the sensitivity of the probe is not good enough due to the apparent background fluorescence, it represents the first example where PPIase activity has been directly imaged in live cells, and should be inspiring for future work. Given the importance of PPIases in regulating protein conformation and function, we envision that further work may be conducted with the construction of new probes whose spectral properties at *cis* and *trans* geometries could be well resolved and those that have brighter and red-shifted excitation/emission spectra.

All methodology procedures are detailed in the ESI.<sup>†</sup>

This work was supported by the National Key Research and Development Program of China (2016YFE0125400), the National Natural Science Foundation of China (81573411 and 21778048), the Natural Science Foundation of Zhejiang Province (LZ16H310001 and LR18H300001), and the Zhejiang Province Program for Cultivation of High-level Health talents.

## Conflicts of interest

There are no conflicts to declare.

## Notes and references

- G. Fischer, *Chem. Soc. Rev.*, 2000, **29**, 119–127.
- K. Lang and F. X. Schmid, *Nature*, 1988, **331**, 453–455.
- K. Lang, F. X. Schmid and G. Fischer, *Nature*, 1987, **329**, 268–270.
- G. Fischer and F. X. Schmid, *Biochemistry*, 1990, **29**, 2205–2212.
- C. Scholz, J. Rahfeld, G. Fischer and F. X. Schmid, *J. Mol. Biol.*, 1997, **273**, 752–762.
- J. Fanghanel and G. Fischer, *Front. Biosci.*, 2004, **9**, 3453–3478.
- A. Bell, P. Monaghan and A. P. Page, *Int. J. Parasitol.*, 2006, **36**, 261–276.
- L. J. Blair, J. D. Baker, J. J. Sabbagh and C. A. Dickey, *J. Neurochem.*, 2015, **133**, 1–13.
- S. D. Hanes, *Biochim. Biophys. Acta*, 2015, **1850**, 2017–2034.
- P. E. Shaw, *EMBO Rep.*, 2007, **8**, 40–45.
- Q. Yao, M. Li, H. Yang, H. Chai, W. Fisher and C. Chen, *World J. Surg.*, 2005, **29**, 276–280.
- L. McClements, S. Annett, A. Yakkundi and T. Robson, *Curr. Mol. Pharmacol.*, 2015, **9**, 165–179.
- L. Pastorino, A. Sun, P. J. Lu, X. Z. Zhou, M. Balastik, G. Finn, G. Wulf, J. Lim, S. H. Li, X. Li, W. Xia, L. K. Nicholson and K. P. Lu, *Nature*, 2006, **440**, 528–534.
- T. H. Lee, L. Pastorino and K. P. Lu, *Expert Rev. Mol. Med.*, 2011, **13**, e21.
- R. Thapar, *Biomolecules*, 2015, **5**, 974–999.
- B. Janowski, S. Wollner, M. Schutkowski and G. Fischer, *Anal. Biochem.*, 1997, **252**, 299–307.
- Y. J. Jin, S. J. Burakoff and B. E. Bierer, *J. Biol. Chem.*, 1992, **267**, 10942–10945.
- J. A. Prescher and C. R. Bertozzi, *Nat. Chem. Biol.*, 2005, **1**, 13–21.
- J. A. Gonzalez-Vera and M. C. Morris, *Proteomes*, 2015, **3**, 369–410.
- K. M. Dean and A. E. Palmer, *Nat. Chem. Biol.*, 2014, **10**, 512–523.
- Y. Hori, K. Nakaki, M. Sato, S. Mizukami and K. Kikuchi, *Angew. Chem., Int. Ed.*, 2012, **51**, 5611–5614.
- G. Zoldak, T. Aumuller, C. Lucke, J. Hritz, C. Oostenbrink, G. Fischer and F. X. Schmid, *Biochemistry*, 2009, **48**, 10423–10436.
- C. Mas, I. Guimiot-Maloum, F. Guimiot, M. Khelfaoui, V. Nepote, F. Bourgeois, B. Boda, B. Levacher, A. Galat, J. M. Moalic and M. Simonneau, *Gene Expression Patterns*, 2005, **5**, 577–585.
- G. L. Perrucci, A. Gowran, M. Zanobini, M. C. Capogrossi, G. Pompilio and P. Nigro, *Cardiovasc. Res.*, 2015, **106**, 353–364.